Michigan Technological University

Digital Commons @ Michigan Tech

Michigan Tech Publications

An improved electron pre-sheath model for TSS-1R current enhancement computations

Chunpei Cai

Tethered Satellite Systems (TSS) can be deployed for a variety of important applications, including electro-dynamic propulsion, momentum exchange, tidal stabilization, artificial gravity, deployment of sensors or antennas, and orbital plasma dynamics [1]. They are helpful to investigate characterizations of the system current–voltage (I–V) response in the ionosphere plasma environment, the characterization of the physics of the satellite sheath, or current collection, and of overall current closure. The orbital motion through the Earth's geomagnetic field allows orbiting tethered systems to generate a much higher electromotive force [2]. Especially, spacecraft charging is a serious and practical concern in space engineering, and there have been extensive research activities aimed to address these issues. Among all approaches, tethering systems are quite effective to investigate the charging [3] and magnetic field effects [4], and there are some recent review papers in the literature [1,5–7].

The TSS-1R is a shuttle-based system [8,9] jointly developed and operated by NASA and the Italian Space Agency. It consists of a spherical satellite tethered by a space shuttle with a 21.7 km of conducting tether with a total of resistance of 2100 ohms. The satellite traveled with a speed of 7800 m/s, roughly an order of magnitude faster than a sounding rocket payload. The satellite has higher potential than the ambient ionosphere, and electrons are collected onto the satellite, as the spacecraft charging process. An extra electron current is passed to the shuttle from the satellite. The tests were performed in 1996, however, the currents measured [2,10] were reported to be factors of two or three times greater than the predictions of the convectional Parker-Murphy (P-M) model and theory [4]. This result was rather surprising since the P-M theory provides an upper limit for current collection. It is well known, that conventional sheath models are not complete without a treatment of the pre-sheath model that matches the sheath edge conditions to the ambient plasma.

On the scale of the TSS, the surrounding plasma is collisionless and the ambient electron gyro-radius is small; hence, it would seem that the TSS should deplete the immediate flux tube of

electrons. If the tube was refilled along a length on which the plasma can be considered collisional [11], it is unclear whether the tube could carry a full thermal current to the sheath surface as assumed by the P-M theory. There are experimental data suggesting that the flux tubes indeed carry the full electron thermal flux to the sheath edge. Although many electron beam-emitting rockets have observed return currents in excess of the P-M limit, it was demonstrated by the Cooperative High Altitude Rocket Gun Experiment (CHARGE) II experiment that this effect was due to the beam [12]. Here, the electron-emitting mother payload experienced a return current in excess of the P-M limit, while the tethered daughter did not [13]. The Spectroscopy of Plasma Evolution from Astrophysical Radiation (SPEAR) I experiment also observed electron collection consistent with magnetic limiting in the high voltage sheath of a positively-biased probe [14].

These sounding rocket experiments demonstrate that for even near stationary collections, the ionosphere can refill the flux tube near the sheath. Understanding how this refilling occurs is an important part of magnetic probe theory [15,16], and the ultimate source of the electrons constitutes the current closure issue [17]. In recent years, there are still investigations on the positive probe problems. For example, Singh [18] simulated the plasma flows around the TSS-1R and compared with the experimental measurements in space; Heinrich and Cooke [19] simulated ae problem of plasma flows around a positive probe with the Particle-In-Cell (PIC) method. However their simulations are three-dimensional, and quite time-consuming. By comparison, analytical and semi-analytical formulas can offer clear physics and the evaluation speeds can be quite fast. Cooke and Katz [20] argued that separating the issues of current closure and the current collection is empirically justified. They constructed a local probe model assuming an undisturbed plasma exists on the boundary of the iteration. Their results are concise, and affected the NASA guidelines for spacecraft designs [21].

This paper presents improvements on their previous work [20], with more rigorous mathematical treatments on the pre-sheath model and more measurements are included.

2. Background for Positive Probe Sheath and Current

The disturbed region of plasma surrounding a high voltage probe is commonly dissected into sheath and pre-sheath regions. There are three basic sheath models, "Orbit limited", "Space charge limited", and "Magnetic (P-M) limited" [4]. The last one is the model of our concerns due to the Earth's strong magnetic field. In the ionosphere, electron gyration radii are on the order of centimeters, satellite dimensions are on the order of meters, and collision mean free paths are on the order of kilometers. As such, electrons move along the Earth's magnetic field lines, but remain essentially "glued" to the field lines with tight spiral motions around them. Parker and Murphy (1967) [4] observed that for a potential distribution symmetrical about the magnetic field, the conservations of canonical angular momentum and energy yield a maximum cylindrical radius, R_{PM}, from which an electron may reach the probe surface. This radius defines a flux tube from which electrons may be collected, and leads to a limiting current after specifying the current density in the flux tube. The P-M limit is weak because it can be violated by fluctuations [22] or lack of symmetry [14]. There are other popular theoretical models (e.g., the one developed by Albert [23]) for spherically isotropic collections and collisionless conditions, in the absence of a magnetic field, but in the TSS-1R mission, the flow regime was never reached, and those other models are not discussed here.

Whether the probe current is P-M or space-charge limited can be estimated by forming the ratio, between R_{LB} and R_{PM}, where the former is the sheath by Langmuir-Blodgett [3]. When the ratio is larger than 1, the collection is P-M limited, and the space charge of electrons with R_{PM} does not completely shield the probe. The probe potential therefore extends beyond R_{PM}, creating a region to which electrons are attracted but from which they cannot be collected. Even though these electrons are energetically capable of escaping, they cannot easily find an exit vector and form an $E \times B$ drifting shell of quasi-trapped electrons. Self-consistent modeling and laboratory experiments in support of the SPEAR I experiment demonstrate that this layer of circulating charges mostly overlies the P-M sheath region with negligible extension beyond R_{PM}. This contributes additional space charges and

confines the sheath close to the PM radius. Figure 1 illustrates this region. The actual trajectories of the quasi-trapped electrons reach from this shell to just above the probe surface.
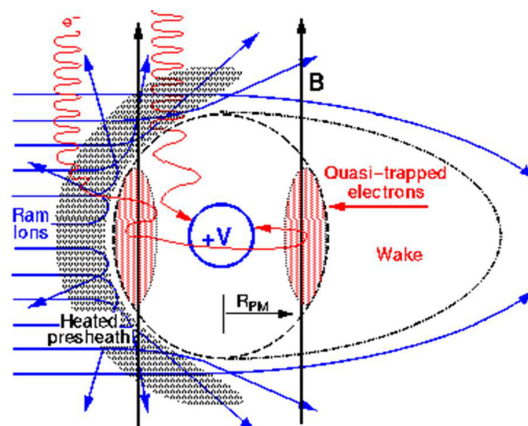

Figure 1. Schematic illustration of the interaction model [20].

3. Different Approaches for Pre-Sheath Modeling

One most important finding from the TSS-1R mission was that the Parker-Murphy theory significantly under-predicted the collected electron current. It was argued that the sheath model is not enough to describe the problem, and the pre-sheath model must be considered as well. Figure 2 illustrates the relation across the pre-sheath, which is simplified as one-dimensional.
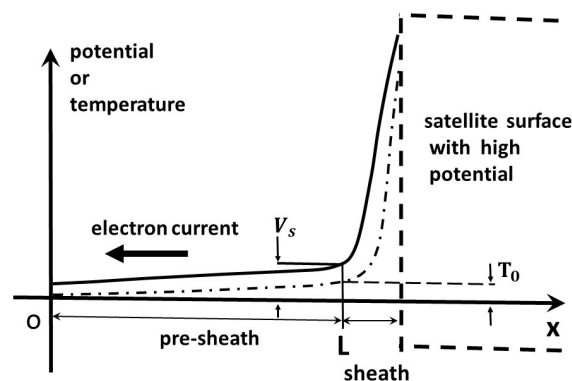
Figure 2. Illustration for the pre-sheath model.

Across the pre-sheath, behind the shock wave but in front of a sphere, there are two relations, one is the current and the other is the thermodynamic relation among heat flux, temperature, and current strength [20]:

$$I = \nabla V - \frac{1}{n}\nabla(nT) \approx \nabla V - \nabla T, \tag{1}$$

$$Q = -\frac{3}{2}T\nabla T + \frac{5}{2}TI, \tag{2}$$

where I is current density, T is electron temperature, V is plasma potential, n is electron or plasma density, and Q is heat flux. Equation (1) assumes that the normalized electron number density gradient is negligible across the pre-sheath.

The current continuity and heat relations are:

$$\nabla \cdot I = 0; \nabla \cdot Q = I^2. \tag{3}$$

The first relation was discarded in their work due to the poor final agreements with measurements in the mission. From the other expression, the following relation linking the temperature and potential changes is developed:

$$\nabla^2 V = \nabla^2 T, \tag{4}$$

a solution for the above relation is $\nabla V = \nabla T - c_0$, where c_0 is a constant vector. The energy relations, Equations (2) and (3), transform into the following format:

$$5\,(\nabla T)^2 - \frac{9}{2}\nabla T \cdot \nabla V + (\nabla V)^2 + \frac{3}{2}T\nabla^2 T = 0. \tag{5}$$

The past approach by Cooke and Katz [20]. If the second order gradient term in Equation (5) is neglected, then there are two solutions:

$$\nabla T = \frac{1}{2}\nabla V, \nabla T = \frac{2}{5}\nabla V, \tag{6}$$

The flow is simplified as one-dimensional, and by using the following important mathematical integration relation:

$$\int_0^1 \sqrt{1 + ax^2}dx = \frac{1}{2}\sqrt{1 + a} + \frac{1}{2\sqrt{a}}\ln(\sqrt{a} + \sqrt{1 + a}), \tag{7}$$

the final general expression for the pre-sheath current due to thermal motion is obtained:

$$I_{PS}/(2\pi R_{PM}^2 I_0) = \frac{1}{2}\left(1 + (1 + \chi)^{1/2} + \chi^{-1/2}\ln(\chi^{1/2} + (1 + \chi)^{1/2})\right), \tag{8}$$

where $\chi \equiv (T_s - T_0)/T_0$, T_s and T_0 are the electron temperatures at the starting and ending of the pre-sheath. As the parameter χ increases, the current through the pre-sheath can be further simplified as [20]:

$$I_{PS}/(2\pi R_{PM}^2 I_0) = \frac{1}{2}\left(1 + (1 + \chi)^{1/2}\right). \tag{9}$$

A new approach. The above treatment can be improved and one of the major purposes of this paper is to report this new treatment. One small defect in the above approach is that Equation (6) is inconsistent with Equation (4). With careful deviations, Equation (5) can transform to the following format if the higher order gradient term is reserved:

$$(7\nabla T - 2\nabla V) \cdot (\nabla T - \nabla V) + 3\nabla \cdot (T\nabla T) = 0. \tag{10}$$

At the start of the pre-sheath, there are two boundary conditions, $T(0) = T_0$, and $V(0) = 0$. If the probe potential is high enough, then the potential at the sheath edge takes specific values, $V(x = L) = V_s = 0.493$ eV [24]. The temperature at the sheath edge is to be determined.

It can be shown, if the current is zero, $I = 0$, then there are two specific solutions to the potential and temperature:

$$V(x) = \sqrt{\frac{V_s(V_s + 2T_0)}{L}x + T_0^2} - T_0; T(x) = \sqrt{\frac{V_s(V_s + 2T_0)}{L}x + T_0^2}, \tag{11}$$

and Equation (4) holds. The above solutions imply that there is no current across the pre-sheath, based on Equation (1).

　　　Equations (4) and (5) can be simplified as two ordinary differential equations for a one-dimensional situation, and further can be merged into an ordinary Abel differential equation of the second kind [25]. With proper boundary conditions, there are exact mathematical solutions, however, the solutions are rather complex for use and are not adopted in this work. The following simpler approach is developed instead, and they transform the ordinary differential equation into an algebraic equation.

　　　First the *X*-coordinate for Equations (4) and (5) is normalized by using the pre-sheath length, and the domain of interest transforms into $0 \leq X \leq 1$. A new variable for the temperature is defined as $t(X) = T(X) - T_0$, with the boundary values $t(X = 0) = 0$ and $t(X = 1) = t_s = T_s - T_0$, where the latter is the property of our interest. Then, Equation (4) transforms as:

$$\nabla^2 v(X) = \nabla^2 t(X), \tag{12}$$

which has a general solution $v(X) = t(X) + c_0 X + c_1 = t(X) + c_0 X$. With these transformations, Equation (5) changes to:

$$5(\nabla t)^2 - \frac{9}{2}\nabla t \cdot \nabla v + (\nabla v)^2 + \frac{3}{2}(t + T_0)\nabla^2 t = 0. \tag{13}$$

This equation can further transform if we introduce one new variable, $\alpha \equiv t_s/v_s > 0$, with $c_0 = v_s - t_s = (1 - \alpha)v_s$, then

$$\left(\frac{3}{2}\nabla t - \frac{1-\alpha}{\alpha}t_s\right)\left(\nabla t - \frac{1-\alpha}{\alpha}t_s\right) + \frac{3}{2}(t + T_0)\nabla^2 t = 0. \tag{14}$$

　　　Across the pre-sheath, $0 \leq \alpha \leq \infty$, its value is bounded, because there are always finite potential and voltage changes.

　　　Enlightened by the solution format developed by Cooke and Katz [20], the following general power function format for $t(X)$ is assumed, with which the above ordinary differential equation can degenerate to an algebraic equation:

$$t(X) = t_s X^n, \tag{15}$$

where *n* is a free parameter, limited between 0 and 1, which mimics the quadratic formats in Equations (6) and (11). At the sheath ending edge, with $X = 1$, Equation (14) simplifies as:

$$\frac{1}{\alpha^2} - \left(\frac{5}{2}n + 2\right)\frac{1}{\alpha} + \frac{3}{2}n(n-1)\frac{1}{\alpha}\frac{T_0}{v_s} + 3n^2 + n + 1 = 0. \tag{16}$$

　　　If $n > 1$, there is no real solution for the above equation. This fact is compatible with our assumptions on the scope for the parameter range. There are two real roots of α for the above equation, and Figure 3 shows the results varying with different *n* values, where parameters $T_0 = 0.13$ ev, $v_s = 0.493$ V are used in the above equation. These two parameters are the reference values for the TSS-1R mission performed in the ionosphere. This figure illustrates that: (1) in the lower branch, α is less sensitive to *n* when α is small, and there is an asymptote of 0.4 when *n* approaches to unity; (2) it is evident that the past results by Cooke and Katz [20] are consistent, they are special scenarios to the new general solutions developed here; (3) the branch with larger α changes relatively quickly, and it approaches to 0.5 when *n* approaches to 1.

　　　Figure 4 shows two current enhancement coefficients related with the small α branch in Figure 3 (represented with the dashed line). The two branches in Figure 4 correspond to the right hand side terms in Equations (8) and (9). $T_0 = 0.13$ ev and $v_s = 0.493$ volts are used as the parameters in Equation (16) for computations. As shown, very mild changes in the enhancement factors are observed as *n* increases. The simplified current enhancement coefficient is smaller than the non-simplified coefficient. When *n* is close to 1, the specific enhancement coefficient is 2.5; which is very close to the past value adopted by Cooke and Katz [20].
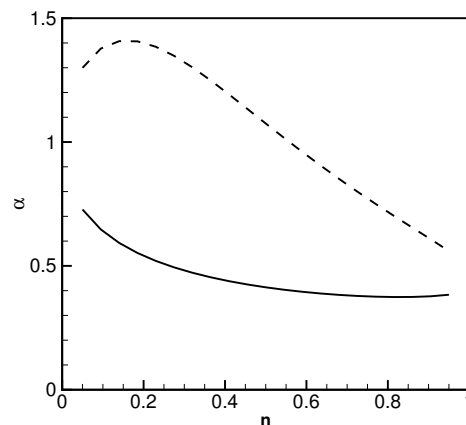
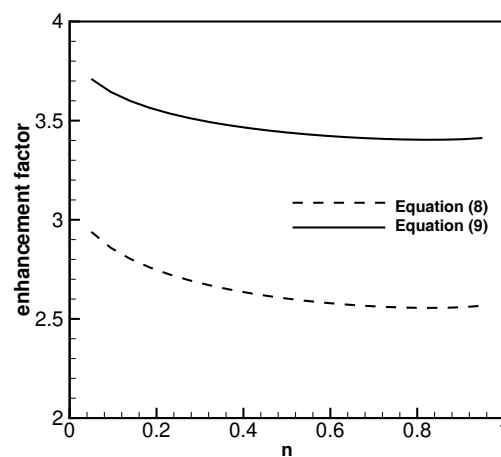**Figure 3.** Two α roots for different n values.

Figure 4. Current enhancement coefficients corresponding to the small α value (represented by the solid and black line in Figure 3).

Figure 5 shows additional experimental results collected in the TSSR-1R mission [26] with different free stream conditions. Nanvario et al. [26] adopted a group of averaged free stream parameters, and computed a smooth curve for the Parker-Murphy theory [4,8]:

$$\frac{I}{I_0} = \frac{1}{2} + \sqrt{\frac{V}{V_0}}, \quad \text{where} \quad I_0 = \pi a^2 en\sqrt{\frac{8kT_e}{\pi m_e}}; V_0 = \frac{B^2 a^2 e}{2m_e}, \tag{17}$$

where V is the measured voltage, $B = 0.32$ Gauss is the Earth's magnetic field strength, a is the radius for the spherical satellite, e is the electron change, n is the ambient electron density, T_e and m_e are the electron temperature and mass. That curve is included in this figure as a long dashed line at the bottom. Space experimental measurements collected during the TSS-1R mission are represented by circles, and the best fitted curve is presented as the solid black line. These data are very valuable because they reflect plasma behaviors in the ionosphere, and can not be created in a ground environment. It is evident that there are large scatters because the data are collected within different time periods, and with slightly different free stream electron temperatures T_0, and different values for number density n. Two current enhancement curves are computed and included in this figure as two dash-dotted lines, the computations are based on Equations (8) and (9), the specific values are computed by averaging the enhancement values within the range of $0.5 < n < 1.0$ in Figure 4. The large scatters in the experiments indicate it is impossible to use one curve to describe these data. However, these two new curves for

current enhancement coefficient bound most measurements, and successfully captured the trends in the experimental data. They are more accurate than the traditional P-M theory. The past work [20] adopted a specific enhancement factor with one curve, and included only seven measurement data points available at the time when the paper was published. The single curve represents the seven measurement points very well, more experiments are available now, and they indicate that one curve cannot represent the results very well. Figure 5 also includes a solid red line which is computed by averaging these two new lines. Evidently, the averaged curve agrees quite well with the best curve-fitting results for the experimental measurements.
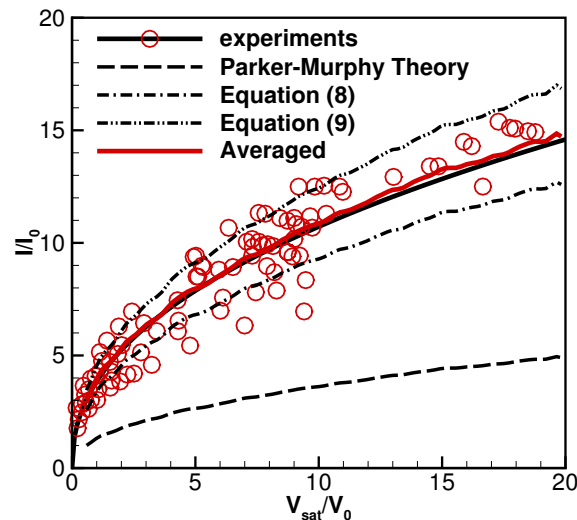
Figure 5. Comparisons of current-voltage results. Symbols: measurements in space mission (solid black line: the best fitting curve); Long dashed line: P-M theory; Black dash-dot lines: new enhancement factors (solid red line: their average).

4. Conclusions

This paper reports improvements on analyzing current enhancements during the TSS-1R mission. A more rigorous mathematical treatment procedure is developed and presented. Compared with the past treatment [20], the second order differential term in the governing partial differential equation is preserved for the pre-sheath model. By assuming special formats for the temperature profiles within the pre-sheath, a family of general, exact solutions to the partial differential equation are obtained. The results indicate that a smaller α value is more reasonable. The n values in this new model do not lead to appreciable differences in the predicted current enhancement results. The work also confirms the past treatment [20] is a special case with $n = 1$, and the past work is reasonable and solid.

In the past effort [20], seven data points were included for comparison. The data agree well with their formula, and predicted a current enhancement coefficient of 2.5. This study includes more experimental measurements and recovers a new curve. The large scatters in the measured TSS-1R space mission indicate that it is challenging to describe the measurements by using one curve. Instead, the two curves developed in this study properly bound the measurements. The curve computed by averaging these two curves agrees surprisingly well with the best curve-fitting results for the experimental measurements. The averaged current enhancement coefficient is estimated as 2.95, which is slightly larger than 2.5, as recommended by Cooke and Katz [20].

Conflicts of Interest: The author declares no conflict of interest.

References

1. Chen, Y.; Huang, R.; Ren, X.; He, L.; He, Y. History of the tether concept and tether missions: A review. *ISRN Astron. Astrophys.* **2013**, doi:10.1155/2013/502973.

2. Wright, K.H.; Stones, N.H.; Winningham, J.D; Curgiolo, D.; Bonifazi, D.; Gilchrist, B.; Dobrowolny, M.; Mariani, F.; Hardy, D. Satellite particle collection during active states of the tethered satellite collection during active states of the tethered satellite system (TSS). In Proceedings of the 27th AIAA Plasma-Dynamics and Lasers Conference, New Orleans, LA, USA, 17–20 June 1996; AIAA Paper 1996–2298.

3. Langmuir, I.; Blodgett, K.B. Currents limited by space charge between concentric spheres. *Phys. Rev.* **1924**, *24*, 49–59.

4. Parker, L.W.; Murphy, B.L. Potential buildup on an electron emitting ionospheric satellite. *J. Geophys. Res.* **1967**, *72*, 1631–1636.

5. Sanmartin, J.R. A review of electrodynamic tethers for science applications. *Plasma Sources Sci. Technol.* **2010**, *19*, 034022.

6. Snamartin, J.R.; Lorenzine, E.C.; Martinez-Sanchez, M. Electrodynamic tether applications and constraints. *J. Spacecr. Rockets* **2010**, *47*, 442–456.

7. Cartmell, M.R.; McKenzie, D.J. A review of space tether research. *Prog. Aerosp. Sci.* **2008**, *44*, 1–21.

8. Dobrowolny, M.; Stone, N.H. A technical overview of TSS-1: The first tethered satellite mission. *Nuovo Cimento* **1994**, *17*, doi:10.1007/BF02506678.

9. Dobrowolny, M.; Melchioni, E. Electrodynamic aspects of the first tethered satellite mission. *J. Geophys. Res.* **1993**, *98*, 13761–13778.

10. Thompson, D.C.; Bonifazi, C.; Gilchrist, B.; Williams, S.D.; Raitt, W.J.; Lebrton, J.P.; Burke, W.J.; Stone, N.H.; Wright, K.H. The current-voltage characteristics of a large probe in low Earth orbit: TSS-1R results. *Geophys. Res. Lett.* **1997**, *25*, 413–416.

11. Sanmartin, J.R. Theory of a probe in a strong magnetic field. *Phys. Fluids* **1970**, *13*, 103–116.

12. Myers, N.B.; Raitt, W.J.; Gilchrist, B.; Banks, P.U.; Neubert, T.; Williamson, P.R.; Saski, A. A comparison of current-voltage relation of collectors in the Earth's ionosphere with and without electron beam emission. *Geophy. Res. Lett.* **1989**, *16*, 365–368.

13. Mandell, M.J.; Lilley, J.R.; Katz, I.; Neubert, T.; Myers, N.B. Computer modeling of current collection by the CHARGE-2 mother payload. *Geophys. Res. Lett.* **1990**, *16*, 135–138.

14. Katz, I.; Jongeward, G.A.; Davis, V.A.; Mandell, M.; Kuharshi, R.A.; Lilley, J.R.; Raitt, W.J.; Cooke, D.L.; Torbert, R.B.; Larson, G.; et al. Structure of the bipolar plasma sheath generated by SPEAR I. *J. Geophys. Res.* **1989**, *94*, 1450.

15. Laframboise, J.G.; Sonomer, L.J. Current collection by probes and electrodes in space magneto-plasma: A review. *J. Geophys. Res.* **1993**, *98*, 337–357.

16. Laframboise, J.C. Current collection by a positively charged spacecraft: Effect of its magnetic pre-sheath. *J. Geophys. Res.* **1997**, *102*, 2417–2432.

17. Stenzel, R.L.; Urrutiz, J.M. Transient current collection and closure for a laboratory tether. *Geophys. Res. Lett.* **1997**, *25*, doi:10.1029/98GL00225.

18. Singh, N.; Leung, W.C.; Singh, G.M. Enhanced current collection by a positively charged spacecraft. *Geophys. Res. Space Phys.* **2000**, *105*, 20935–20947.

19. Heinrich, J.R; Cooke, D.L. Dynamics of positive probes in under-dense, strongly magnetized, E × B drifting plasma: Particle-In-cell simulations. *Phys. Plasmas* **2013**, *20*, doi:10.1063/1.4821070.

20. Cooke, D.; Katz, I. TSS-1R electron currents: Magnetic limited collection from a heated pre-sheath. *Geophys. Res. Lett.* **1998**, *25*, 736–756.

21. Ferguson, D.; Hillard, G.B. Low Earth Orbit Spacecraft Charging Design Guidelines. In Proceedings of the 8th Spacecraft Charging Technology Conference, NASA Marshall Space Flight Center, Huntsville, AL, USA, 20–24 October 2003; NASA/TP-2003-212287.

22. Linson, L.M. Current-voltage characteristic of an electron-emitting satellite in the ionosphere. *J. Geophys. Res.* **1969**, *74*, 2368–2375.

23. Alpert, Y.L.; Gurevich, A.V.; Pitaewskii, L.P. Disturbance of the plasma and the electric field in the vicinity of a charged body at rest. In *Space Physics with Artificial Satellites*; Consultant Bureau, New York, NY, USA, 1965; p. 186.

24. Parrot, M.J.M.; Storey, L.R.O.; Parker, L.W.; Laframboise, J.G. Theory of cylindrical and spherical Langumir probe in the limit of vanishing Debye number. *Phys. Fluids* **1982**, *25*, 2388.

25. Colton, D.; Kress, R. *Integral Equation Methods in Scattering Theory*; John Wiley: New York, NY, USA, 1983.

26. Vannaroni, G.; Dobrowony, M.; Lebreton, J.P.; Melchioni, E.; Venuto, F.D.; Harvey, C.C.; Less, L.; Guidoni, U.; Bonifazi, C.; Mariani, F. Current-voltage characteristic of the TSS-1R satellite: Comparison with isotropic and an-isotropic models. *Geophys. Res. Lett.* **1998**, *25*, 749–752.